IIE Transactions (2004) **36**, 807–815

ISSN: 0740-817X print / 1545-8830 online
DOI: 10.1080/07408170490472999

Variation transmission analysis and diagnosis of multi-operational machining processes

QIANG HUANG[1] and JIANJUN SHI[2*]

[1] *Department of Industrial and Management Systems Engineering, University of South Florida, Tampa, FL 33620, USA*
E-mail: huangq@eng.usf.edu
[2] *Department of Industrial and Operations Engineering, The University of Michigan, Ann Arbor, MI 48109, USA*
E-mail: shihang@umich.edu

Received November 2001 and accepted June 2003

In a Multi-operational Machining Process (MMP), final product variation is an accumulation, or stack-up of variations generated at all the manufacturing operations. In this paper, variation transmission in the MMP is analyzed by relating part variations to operational errors from machine tools, fixtures and datums. At each operation, total part variation is separated into several components corresponding to different variation sources. The result can be applied in both process design and diagnosis. A methodology is developed to identify faulty operations. Process diagnosability is also discussed. A case study is provided to illustrate the developed diagnostic methodology.

Nomenclature

$\mathbf{e}_k^{\mathrm{f}}, \mathbf{e}_k^{\mathrm{d}}, \mathbf{e}_k^{\mathrm{m}}$	=	fixture errors, datum errors, and machine tool errors at operation k;
$\mathbf{w}(k), \mathbf{v}(k)$	=	noise terms at operation k;
$\mathbf{X}(k)$	=	a vector to describe part surfaces after operation k, represented in the Part Coordinate System (PCS);
$\mathbf{Y}(k)$	=	quality characteristics generated after operation k;
$\mathbf{x}(k)$	=	deviation of $\mathbf{X}(k)$, represented in the PCS;
$\mathbf{y}(k)$	=	deviation of $\mathbf{Y}(k)$, represented in the PCS;
$\mathbf{B}(k)$	=	indicator matrix which labels all surfaces that are machined at operation k;
$\mathbf{A}(k)$	=	defined as $\mathbf{A}(k) = \mathbf{I} - \mathbf{B}(k)$, indicating surfaces not machined at operation k;
$\mathbf{C}(k)$	=	sensitivity matrix mapping $\mathbf{x}(k)$ to $\mathbf{y}(k)$;
$\mathbf{B}(k)\mathbf{x}^{\mathrm{u}}(k)$	=	newly machined surfaces after operation k, represented in the PCS;
$\mathbf{B}(k)\mathbf{x}_{\mathrm{M}}^{\mathrm{u}}(k)$	=	newly machined surfaces after operation k, represented in the Machine tool Coordinate System (MCS);
${}^{i}\mathbf{R}_{j}(k)$	=	rotation transformation from j to i at operation k, where i, j represent the PCS, Fixture Coordinate System (FCS), or MCS;
${}^{i}\mathbf{T}_{j}(k)$	=	translation transformation from j to i at operation k where i, j represent the PCS, FCS, or MCS;
Z^{o}	=	nominal value of any variable Z, e.g., ${}^{\mathrm{P}}\mathbf{R}_{\mathrm{F}}^{\mathrm{o}}(k)$ denotes the nominal rotation transformation from the FCS to PCS;
ΔZ	=	deviation of variable Z from its nominal value, e.g., $\Delta^{\mathrm{F}}\mathbf{R}_{\mathrm{M}}(k)$ and $\Delta^{\mathrm{M}}\mathbf{T}_{\mathrm{F}}(k)$;
$\mathbf{x}_{\mathrm{M}}, \mathbf{x}_{\mathrm{F}}$	=	deviation of $\mathbf{X}$, represented in the MCS or FCS;
$\boldsymbol{\mu}_Z, \mathbf{K}_Z$	=	mean and covariance of variable Z, e.g., $\boldsymbol{\mu}_{\mathbf{x}^{\mathrm{u}}(k)}$ and $\mathrm{K}_{\mathbf{x}^{\mathrm{u}}(k)}$;
$\mathbf{K}_k$	=	overall part variation after operation k;
$\mathbf{B}(k)\mathbf{K}_{\mathbf{x}^{\mathrm{u}}(k)}\mathbf{B}^T(k)$	=	variation in newly machined surface after operation k;
$\mathbf{\Pi}_k^{\mathrm{m}}, \mathbf{\Pi}_k^{\mathrm{f}}, \mathbf{\Pi}_k^{\mathrm{d}}$	=	components of variation $\mathbf{B}(k)\mathbf{K}_{\mathbf{x}^{\mathrm{u}}(k)}\mathbf{B}^T(k)$ caused by $\mathbf{e}_k^{\mathrm{m}}$, $\mathbf{e}_k^{\mathrm{f}}$, and $\mathbf{e}_k^{\mathrm{d}}$ respectively;
$\mathbf{K}_{\mathbf{w}(k)}$	=	natural process variation at operation k;
$\mathbf{K}_{\mathbf{y}(k)}$	=	variation in quality characteristics after operation k;
$\mathbf{D}(k)$	=	datum selection matrix for choosing the datum for operation k;
$\mathbf{x}'(k), \mathbf{y}'(k)$	=	deviation of part and quality characteristics after virtual operation k.

*Corresponding author

1. Introduction

Variation transmission is a very complicated issue in a Multi-operational Machining Process (MMP). The complexity is primarily due to two reasons: (i) each operation has three major variation sources, i.e., machine tools, fixtures and workpiece, which affect part quality through different ways; and (ii) the operation sequence can make a significant difference in final product variations. This second fact can be explained by the datum effect, i.e., if previous machined features are used as data in the current operation, data imperfection often affects the accuracy of the currently machined features. Consequently, the issue of variation transmission in a MMP needs to be addressed at both the operation level and the process level.

Statistical Process Control (SPC) is a systematic tool to reduce process variations. However, for multistage manufacturing processes, such as MMPs, control charts need to be developed for every single stage so as to determine faulty stage(s). Furthermore, SPC does not focus on variation transmission analysis and root-cause diagnosis. Zhang (1984) proposed cause-selecting control charts to identify out-of-control stages (refer to the review and analysis of Wade and Woodall (1993)). The first step in constructing the chart is to establish the relationship between the incoming workpiece and the outgoing quality characteristics. The proposed chart is then constructed based on the values of the outgoing quality characteristics that have been adjusted for the values of the incoming workpiece. Agrawal *et al.* (1999) and Lawless *et al.* (1999) used an AR(1) model to analyze the variation transmission in multistage manufacturing processes. Cause-selecting control charts and AR(1) modeling are primarily data-driven approaches, that depend on the available historical data.

An understanding of the physics of variation transmission has motivated research on establishing engineering models for MMPs. Most of the related studies have focused on modeling and reducing errors at the operation level. In the field of machine tool error compensation, kinematic modeling of geometric machine tool errors was provided by Anjanappa *et al.* (1988). Chen *et al.* (1993) presented a more complicated time-variant volumetric model. As to the fixture variation analysis, Weil *et al.* (1991) analyzed datum positional errors. Rong and Bai (1996) verified fixture locating schemes by considering machining accuracy. Cai *et al.* (1997) developed a variational method to conduct robust fixture design to minimize the workpiece positional errors. Choudhuri and De Meter (1999) considered the contact geometry between the locators and workpiece to investigate the impact of fixture tolerance schemes on datum establishment errors.

Variation analysis at the process level is commonly seen in tolerance design. A variety of tolerance stack-up models have been studied (Chase and Greenwood, 1988). However, assumptions are usually made on the distributions of component dimensions without thorough variation analysis at the operation level. Shi and Jin (1997) and Jin and Shi (1999) developed state-space models to depict variation propagation in assembly processes, in which the impacts of workpiece imperfection and fixture errors on product quality were explicitly explored. That model can be applied for both variation prediction and root-cause diagnosis. By developing a state transition model, Mantripragada and Whitney (1999) modeled the entire assembly sequence as a set of discrete events to simulate and predict the propagation of variation in mechanical assemblies. In their work, part errors and fixture errors were treated together as a white noise term at each assembly station. However, the state transition model is difficult to apply to diagnose variation induced by fixtures, because part errors and fixture errors are not distinguished in white noise terms. Furthermore, the impact of those two types of errors on product quality was not explicitly modeled. The situation in machining processes is more complex, because there is not only datum error and fixture error, but also machine tool error. It is more challenging to incorporate three types of errors into a process-level error propagation model. Huang *et al.* (2000, 2003) first developed variation propagation model for MMPs. That model was further linearized and studied by Djurdjanovic and Ni (2001). Zhou *et al.* (2003) improved the modeling work in Huang *et al.* (2000, 2003) by using a differential motion vector. Root-cause identification has also been studied for assembly processes (Ceglarek and Shi, 1996; Apley and Shi, 1998; Ding *et al.*, 2002) and machining processes (Huang *et al.*, 2002)

The purpose of this paper is to present an analysis of variation transmission and to apply the result to identify faulty operations based on the modeling work of Huang *et al.* (2000, 2003). The remainder of the paper includes four sections. In Section 2, the variation transmission in MMPs is analyzed after a brief review of the previously developed model. Process diagnosability assessment and faulty operation identification are proposed in Section 3. The diagnostic procedure is shown with a case study in Section 4. Finally, the work is summarized in Section 5.

2. Analysis of variation transmission

2.1. *Review of the state space model for the MMPs*

At operation k of an N-operation machining process, variation sources include fixture error $\mathbf{e}_k^{\mathrm{f}}$, datum error $\mathbf{e}_k^{\mathrm{d}}$, machine tool error $\mathbf{e}_k^{\mathrm{m}}$, and noise $\mathbf{w}(k)$ due to natural process variation (Fig. 1). $\mathbf{e}_k^{\mathrm{f}}$, $\mathbf{e}_k^{\mathrm{d}}$, $\mathbf{e}_k^{\mathrm{m}}$ and $\mathbf{w}(k)$ are assumed to be mutually independent. In Huang *et al.* (2000, 2003), a state space model is developed to describe the part deviation transmission and observation:

$$\begin{aligned}\mathbf{x}(k) &= \mathbf{A}(k)\mathbf{x}(k-1) + \mathbf{B}(k)\mathbf{x}^{\mathrm{u}}(k) + \mathbf{w}(k),\\ \mathbf{y}(k) &= \mathbf{C}(k)\mathbf{x}(k) + \mathbf{v}(k),\end{aligned} \tag{1}$$

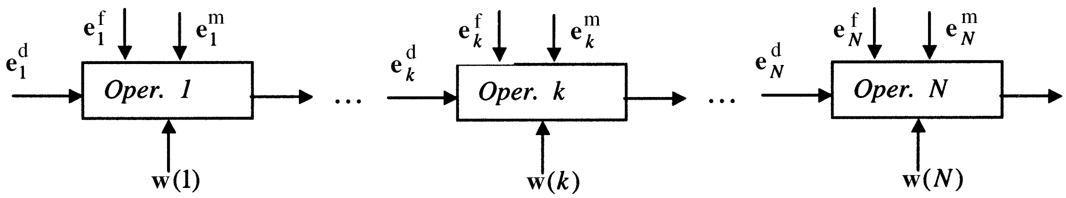

Fig. 1. Error transmission in a MMP.

where $\mathbf{B}(k)\mathbf{x}^{\mathrm{u}}(k)$ is further represented as:

$$\begin{aligned}\mathbf{B}(k)\mathbf{x}^{\mathrm{u}}(k) = {}&{}^{P}\mathbf{R}_{\mathrm{F}}^{\mathrm{o}}(k)^{\mathbf{F}}\mathbf{R}_{\mathbf{M}}^{\mathrm{o}}(k)\mathbf{B}(k)\mathbf{x}_{\mathrm{M}}^{\mathrm{u}}(k)\\ &+\big[{}^{\mathbf{P}}\mathbf{R}_{\mathbf{F}}^{\mathrm{o}}(k)\Delta^{\mathrm{F}}\mathbf{R}_{\mathrm{M}}(k)\mathbf{B}(k)^{\mathrm{M}}\mathbf{R}_{\mathrm{F}}^{\mathrm{o}}(k)^{\mathrm{F}}\mathbf{R}_{\mathrm{P}}^{\mathrm{o}}(k)\mathbf{X}^{\mathrm{o}}(k)\\ &-{}^{\mathrm{P}}\mathbf{R}_{\mathrm{F}}^{\mathrm{o}}(k)^{\mathrm{F}}\mathbf{R}_{\mathrm{M}}^{\mathrm{o}}(k)\mathbf{B}(k)\Delta^{\mathrm{F}}\mathbf{R}_{\mathrm{M}}(k)^{\mathrm{F}}\mathbf{T}_{\mathrm{P}}^{\mathrm{o}}(k)\\ &-{}^{\mathrm{P}}\mathbf{R}_{\mathrm{F}}^{\mathrm{o}}(k)^{\mathrm{F}}\mathbf{R}_{\mathrm{M}}^{\mathrm{o}}(k)\mathbf{B}(k)\Delta^{\mathrm{M}}\mathbf{T}_{\mathrm{F}}(k)\big]\\ &+\big[\Delta^{\mathrm{P}}\mathbf{R}_{\mathrm{F}}(k)\mathbf{B}(k)^{\mathrm{F}}\mathbf{R}_{\mathrm{P}}^{\mathrm{o}}(k)\mathbf{X}^{\mathrm{o}}(k)\\ &-{}^{\mathrm{P}}\mathbf{R}_{\mathrm{F}}^{\mathrm{o}}(k)\mathbf{B}(k)\Delta^{\mathrm{F}}\mathbf{T}_{\mathrm{P}}(k)\big]. \qquad (2)\end{aligned}$$

At the right-hand side (RHS) of Equation (2), the three terms from left to right, are caused by $\mathbf{e}_k^{\mathrm{m}}$, $\mathbf{e}_k^{\mathrm{f}}$ and $\mathbf{e}_k^{\mathrm{d}}$ respectively. Since $\mathbf{e}_k^{\mathrm{m}}$, $\mathbf{e}_k^{\mathrm{f}}$ and $\mathbf{e}_k^{\mathrm{d}}$ are independent, those three terms at RHS of Equation (2) are also independent. This separation is extremely important for the variation analysis.

2.2. *Analysis of variation transmission in a MMP*

The part variation at operation k is expressed as the covariance of vector $\mathbf{x}(k)$, i.e.:

$$\mathbf{K}_k = \mathrm{cov}\,(\mathbf{x}(k))\,. \qquad (3)$$

Assume that $\mathbf{w}(k)$ has a zero mean and covariance $\mathbf{K}_{\mathrm{w}(k)}$, and $\mathbf{w}(k)$ is independent of $\mathbf{x}(k-1), \mathbf{x}(k-2), \ldots$, and $\mathbf{x}(0)$, where $\mathbf{x}(0)$ represents the raw workpiece surface deviation. By Equation (1), we have:

$$\begin{aligned}\mathbf{K}_k = {}&\mathbf{A}(k)\mathbf{K}_{k-1}\mathbf{A}^T(k) + \mathbf{B}(k)\mathbf{K}_{\mathbf{x}^{\mathrm{u}}(k)}\mathbf{B}^T(k)\\ &+ 2\mathbf{A}(k)\mathrm{cov}(\mathbf{x}(k-1), \mathbf{x}^{\mathrm{u}}(k))\mathbf{B}^T(k) + \mathbf{K}_{\mathrm{w}(k)}. \qquad (4)\end{aligned}$$

From their definitions in Huang *et al.* (2000, 2003), $\mathbf{A}(k)$ and $\mathbf{B}(k)$ are block diagonal matrices with the blocks either to be identity or zero matrices. Since the product of two corresponding blocks are zero, we have $\mathbf{A}(k)\mathrm{cov}(\mathbf{x}(k-1), \mathbf{x}^{\mathrm{u}}(k))\mathbf{B}^T(k) = \mathbf{0}$, where "**0**" denotes a zero matrix. Equation (4) is thus simplified as:

$$\mathbf{K}_k = \mathbf{A}(k)\mathbf{K}_{k-1}\mathbf{A}^T(k) + \mathbf{B}(k)\mathbf{K}_{\mathbf{x}^{\mathrm{u}}(k)}\mathbf{B}^T(k) + \mathbf{K}_{\mathrm{w}(k)}. \qquad (5)$$

An expression of $\mathbf{B}(k)\mathbf{K}_{\mathbf{x}^{\mathrm{u}}(k)}\mathbf{B}^T(k)$ can be obtained by taking the covariance at both sides of Equation (2). Since the three terms at the RHS of Equation (2) are independent, Equation (5) can be rewritten as:

$$\mathbf{K}_k = \mathbf{A}(k)\mathbf{K}_{k-1}\mathbf{A}^T(k) + \prod\nolimits_k^{\mathrm{m}} + \prod\nolimits_k^{\mathrm{f}} + \prod\nolimits_k^{\mathrm{d}} + \mathbf{K}_{\mathrm{w}(k)}, \qquad (6)$$

where $\prod_k^{\mathrm{m}}$, $\prod_k^{\mathrm{f}}$ and $\prod_k^{\mathrm{d}}$ can be expressed as:

$$\prod\nolimits_k^{\mathrm{m}} = \mathrm{cov}\big[{}^{\mathbf{P}}\mathbf{R}_{\mathbf{F}}^{\mathrm{o}}(k)^{\mathbf{F}}\mathbf{R}_{\mathbf{M}}^{\mathrm{o}}(k)\mathbf{B}(k)\mathbf{x}_{\mathrm{M}}^{\mathrm{u}}(k)\big]$$

$$\begin{aligned}\prod\nolimits_k^{\mathrm{f}} = {}&\mathrm{cov}\big[{}^{\mathrm{P}}\mathbf{R}_{\mathrm{F}}^{\mathrm{o}}(k)\Delta^{\mathrm{F}}\mathbf{R}_{\mathrm{M}}(k)\mathbf{B}(k)^{\mathrm{M}}\mathbf{R}_{\mathrm{F}}^{\mathrm{o}}(k)^{\mathrm{F}}\mathbf{R}_{\mathrm{P}}^{\mathrm{o}}(k)\mathbf{X}^{\mathrm{o}}(k)\\ &-{}^{\mathrm{P}}\mathbf{R}_{\mathrm{F}}^{\mathrm{o}}(k)^{\mathrm{F}}\mathbf{R}_{\mathrm{M}}^{\mathrm{o}}(k)\mathbf{B}(k)\Delta^{\mathrm{F}}\mathbf{R}_{\mathrm{M}}(k)^{F}\mathbf{T}_{\mathrm{P}}^{\mathrm{o}}(k)\\ &-{}^{\mathrm{P}}\mathbf{R}_{\mathrm{F}}^{\mathrm{o}}(k)^{\mathrm{F}}\mathbf{R}_{\mathrm{M}}^{\mathrm{o}}(k)\mathbf{B}(k)\Delta^{\mathrm{M}}\mathbf{T}_{\mathrm{F}}(k)\big] \qquad (7)\end{aligned}$$

$$\begin{aligned}\prod\nolimits_k^{\mathrm{d}} = {}&\mathrm{cov}\big[\Delta^{\mathrm{P}}\mathbf{R}_{\mathrm{F}}(k)\mathbf{B}(k)^{\mathrm{F}}\mathbf{R}_{\mathrm{P}}^{\mathrm{o}}(k)\mathbf{X}^{\mathrm{o}}(k)\\ &-{}^{\mathrm{P}}\mathbf{R}_{\mathrm{F}}^{\mathrm{o}}(k)\mathbf{B}(k)\Delta^{\mathrm{F}}\mathbf{T}_{\mathrm{P}}(k)\big].\end{aligned}$$

Remark 1. Equation (6) indicates that the total part variation after operation k can be separated into five components, i.e., the variation of uncut surfaces from previous operations, the variations of machined surfaces due to $\mathbf{e}_k^{\mathrm{m}}$, $\mathbf{e}_k^{\mathrm{f}}$, $\mathbf{e}_k^{\mathrm{d}}$, and the natural process variation. The covariance between the current operation and previous operations is captured by $\prod_k^{\mathrm{d}}$, which is primarily caused by datum error $\mathbf{e}_k^{\mathrm{d}}$. Equation (6) is interpreted as a variation transmission model which relates the part variation to variation sources.

Remark 2. This result is very helpful for design and manufacturing. For example, at the design stage, alternative fixture designs for a certain operation k can be evaluated by checking $\prod_k^{\mathrm{f}}$. By comparing $\mathbf{K}_N$, alternative operational sequences could be assessed based on the minimum variance criteria. It is thus possible to reduce variations and optimize the design variables at the process level, rather than at the operation level.

The variation of part characteristics is expressed as the covariance of vector $\mathbf{y}(k)$, i.e.:

$$\mathbf{K}_{\mathbf{y}(k)} = \mathrm{cov}\,(\mathbf{y}(k))\,, \qquad (8)$$

Assume that $\mathbf{v}(k)$ has zero mean and covariance $\mathrm{K}_{\mathbf{v}(k)}$, and $\mathbf{v}(\cdot)$ is independent of $\mathbf{w}(\cdot)$ and $\mathbf{x}(\cdot)$. By Equation (1), we have:

$$\mathbf{K}_{\mathrm{v}(k)} = \mathbf{C}(k)\mathbf{K}_k\mathbf{C}^T(k) + \mathbf{K}_{\mathrm{v}(k)}, \qquad (9)$$

If only end-of-line observation $\mathrm{Y}(N)$ is available, by Equation (1), we have:

$$\mathbf{y}(N) = \mathbf{C}(N)\mathbf{x}(N) + \mathbf{v}(N). \qquad (10)$$

The solution of the state space equation is

$$\mathbf{x}(N) = \sum_{i=1}^{N} \mathbf{\Phi}(N, i)\mathbf{B}(i)\mathbf{x}^{\mathrm{u}}(i) + \mathbf{\Phi}(N, 0)\mathbf{x}(0) + \sum_{i=1}^{N} \mathbf{\Phi}(N, i)\mathbf{w}(i), \quad (11)$$

$$\mathbf{y}(N) = \sum_{i=1}^{N} \mathbf{C}(N)\mathbf{\Phi}(N, i)\mathbf{B}(i)\mathbf{x}^{\mathrm{u}}(i) + \mathbf{C}(N)\mathbf{\Phi}(N, 0)\mathbf{x}(0) + \varepsilon \quad (12)$$

where matrix $\mathbf{\Phi}(\cdot,\cdot)$ is defined as:

$$\mathbf{\Phi}(N, i) = \mathbf{A}(N)\mathbf{A}(N-1)\cdots\mathbf{A}(i) \quad \text{and} \quad \mathbf{\Phi}(i, i) = \mathbf{I}. \quad (13)$$

Also, $\boldsymbol{\varepsilon}$ is the summation of all modeling uncertainties and noise terms:

$$\varepsilon = \sum_{i=1}^{N} \mathbf{C}(N)\mathbf{\Phi}(N, i)\mathbf{w}(i) + \mathbf{v}(N). \quad (14)$$

Define $\gamma(i)$ as:

$$\gamma(i) = \mathbf{C}(N)\mathbf{\Phi}(N, i). \quad (15)$$

Then Equation (12) is rewritten as:

$$\mathbf{y}(N) = \sum_{i=1}^{N} \gamma(i)\mathbf{B}(i)\mathbf{x}^{\mathrm{u}}(i) + \gamma(0)\mathbf{x}(0) + \varepsilon. \quad (16)$$

Since $\mathbf{x}(0)$, $\mathbf{w}(\cdot)$ and $\mathbf{v}(\cdot)$ are mutually independent, by Equation (16), we have:

$$\mathbf{K}_{\mathbf{y}(N)} = \sum_{i=1}^{N} \gamma(i)\mathbf{K}_i^{\mathrm{u}}\gamma^{\mathbf{T}}(i) + 2\sum_{i=1}^{N}\sum_{j=1}^{i} \gamma(i)\mathbf{B}(i)\mathrm{cov}\,(\mathbf{x}^{\mathrm{u}}(i), \mathbf{x}^{\mathrm{u}}(j))\,\mathbf{B}^{T}(j)\gamma^{\mathbf{T}}(j) + \gamma(0)\mathbf{K_0}\gamma(0)^{T} + \mathbf{K}_{\varepsilon} \quad (17)$$

with $\mathbf{K}_i^{\mathrm{u}} = \prod_i^{\mathrm{m}} + \prod_i^{\mathrm{f}} + \prod_i^{\mathrm{d}}$ $(i = 1, 2, \ldots, N)$.

Remark 3. Equation (17) is interpreted as the observed variation transmission model. Since it is directly related with design specifications, critical operations can be identified based on their impacts on $\mathrm{K}_{\mathbf{y}(N)}$.

Remark 4. There are four terms on the RHS of Equation (17) with the number of operations N fixed once the process design is determined. Although the magnitudes of those four terms can be reduced by using better precision machine tools, fixtures or workpiece, it also increases the manufacturing cost. The second term, however, is determined by process planning. If the surfaces machined in the ith operation are not used as datum at operation j, then $\mathrm{cov}\,(\mathbf{x}^{\mathrm{u}}(i), \mathbf{x}^{\mathrm{u}}(j)) = 0$. Therefore, Equation (17) suggests that, without increasing manufacturing cost, product dimensional variations can be reduced by reducing correlations among operations, i.e., avoiding choosing surfaces machined at previous operations as datums for current operations.

Remark 5. Equation (17) could be used together with Equation (6) to identify faulty operations in MMPs. This is demonstrated in Section 3 with a process-level diagnostics.

3. Faulty operation identification in a MMP

Based on the variation transmission analysis, this section develops a methodology to identify faulty operations in a MMP. Due to the process complexities, faulty operations may not be distinguished from each other. Therefore, the process diagnosability problem is studied in Section 3.1 with discussions on the diagnosable conditions. Section 3.2 presents the concept of virtual machining to isolate variations among operations. Hypothesis testing is applied in Section 3.3 to determine faulty operations.

3.1. *Process diagnosability*

A machining process is called diagnosable if every faulty operation can be uniquely identified based on a given measurement strategies. Clearly, if both the machined surfaces and the machining datums can be measured, the process is diagnosable. However, sometimes the previously used datums are machined or certain surfaces may be machined twice or more. In that case, direct measurements for those datums or surfaces are not available. Hence, the diagnosis is not straightforward.

Three results are derived from the state space model to investigate whether datum loss or multiple cutting on surfaces exist in the process (derivation is omitted). In the following results, $\mathbf{B}(j)$ is the indicator matrix which labels all surfaces that are machined at operation j and $\mathbf{D}(k)$ is the datum selection matrix for choosing the datum for operation k (Huang *et al.*, 2000, 2003). They are block diagonal matrices with each block having dimension $(6 + m)$ by $(6 + m)$, where $(6 + m)$ is the dimension for one surface and m represents the number of size parameter for the surface.

Result 1. If there exists operations k and j with $j > k$ and $k > 1$, satisfying $\mathbf{D}(k)\mathbf{B}(j) \neq 0$, then the datum used at operation k will be machined at operation j.

Result 2. If there exists operations k and j with $j > k$ and $k > 1$, satisfying $\mathbf{B}(k)\mathbf{B}(j) \neq 0$, then some surfaces machined at operation k is machined again at operation j.

Result 3. If there is no datum loss and no multiple cutting on the same surfaces, then:

$$\begin{cases} \mathbf{B}(i)\mathbf{B}(j) = 0 \\ \mathbf{D}(i)\mathbf{B}(j) = 0, \end{cases} \quad \text{for all } i = 1, \cdots, N, \ \text{ and } \ i < j < N. \quad (18)$$

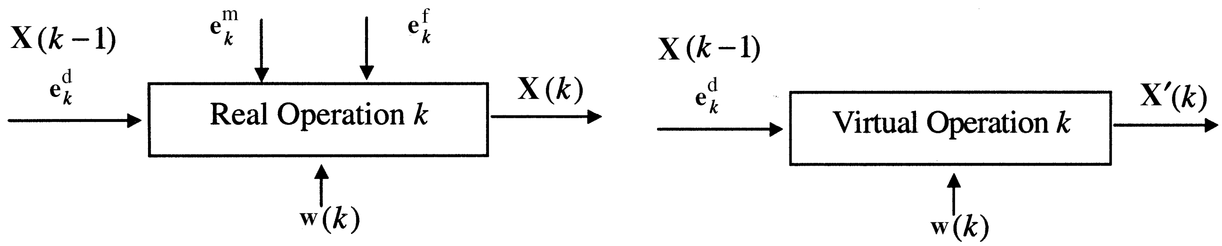

Fig. 2. Virtual operation and real operation.

3.2. *Variation isolation by virtual machining*

If an operation does not use previously machined surfaces as datums, variations of currently machined surfaces are not affected by previous operations. Then the diagnosis can be simplified as a single operation problem. Otherwise, it is necessary to isolate variations among operations so as to identify the faulty operations. The concept of virtual machining is proposed to isolate variations among operations.

Definition 1. Virtual machining in the context of variation isolation is defined as the simulated machining operation based on Equation (1) with extra assumptions that machine tool errors and fixture errors do not exist. At virtual operation k, datum error $\mathbf{e}_k^{\mathrm{d}}$ is the same as that in the real operation k. Denote by $\mathbf{X}'(k)$ the output from virtual operation k (Fig. 2).

By definition 1, the output difference between the virtual operation k and the real operation k is only caused by $\mathbf{e}_k^{\mathrm{m}}$ and $\mathbf{e}_k^{\mathrm{f}}$. Therefore, for a given diagnosable process, the variation isolation can be performed in three steps:

Step 1. Collect measurement data at the final operation and compute statistics. Find out $\mathbf{y}(k)$: $\boldsymbol{\mu}_{\mathbf{y}(k)} = E(\mathbf{y}(k))$ and $\mathrm{K}_{\mathbf{y}(k)} = \mathrm{cov}(\mathbf{y}(k))$.

Step 2. Since the measurement data for machining datums is available, virtual machining can be performed based on the following equations:

$$\mathbf{x}'(k) = \mathbf{A}(k)\mathbf{x}(k-1) + \mathbf{B}(k)\mathbf{x}^{\mathrm{u}'}(k) + \mathbf{w}(k), \quad (19)$$

$$\mathbf{y}'(k) = \mathbf{C}(k)\mathbf{x}'(k) + \mathbf{v}(k). \quad (20)$$

Since $\mathbf{B}(k)\mathbf{x}^{u'}(k)$ is only caused by $\mathbf{e}_k^{\mathrm{d}}$, it can be simplified from using Equation (2) as:

$$\mathbf{B}(k)\mathbf{x}^{\mathrm{u}'}(k) = \Delta^{\mathrm{P}}\mathbf{R}_{\mathrm{F}}(k)\mathbf{B}(k)^{\mathrm{F}}\mathbf{R}_{\mathrm{P}}^{\mathrm{o}}(k)\mathbf{X}^{\mathrm{o}}(k) - {}^{\mathrm{P}}\mathbf{R}_{\mathrm{F}}^{\mathrm{o}}(k)\mathbf{B}(k)\Delta^{\mathrm{F}}\mathbf{T}_{\mathrm{P}}(k) \quad (21)$$

Denote $\boldsymbol{\mu}_{\mathbf{y}'(k)} = E(\mathbf{y}'(k))$ and $\mathbf{K}_{\mathbf{y}'(k)} = \mathrm{cov}(\mathbf{y}'(k))$.

Step 3. By comparing sample statistics of $\mathbf{y}(k)$ and $\mathbf{y}'(k)$, the occurrence of faults can be identified by performing hypothesis testing.

The above procedure can be repeated for operations $N, N-1, \ldots, 2, 1$. As a result, variation isolation among operations can be achieved. Figure 3 shows the concept of variation isolation among operations.

3.3. *Faulty operation identification by hypothesis testing*

Suppose $\mathbf{y}(k)$ $(k \in \{1, 2, \ldots, N\})$ is measurable with n_1 samples, we can compute sample mean $\hat{\boldsymbol{\mu}}_{\mathbf{y}(k)}$ and sample covariance $\mathbf{S}_{\mathbf{y}(k)}$.

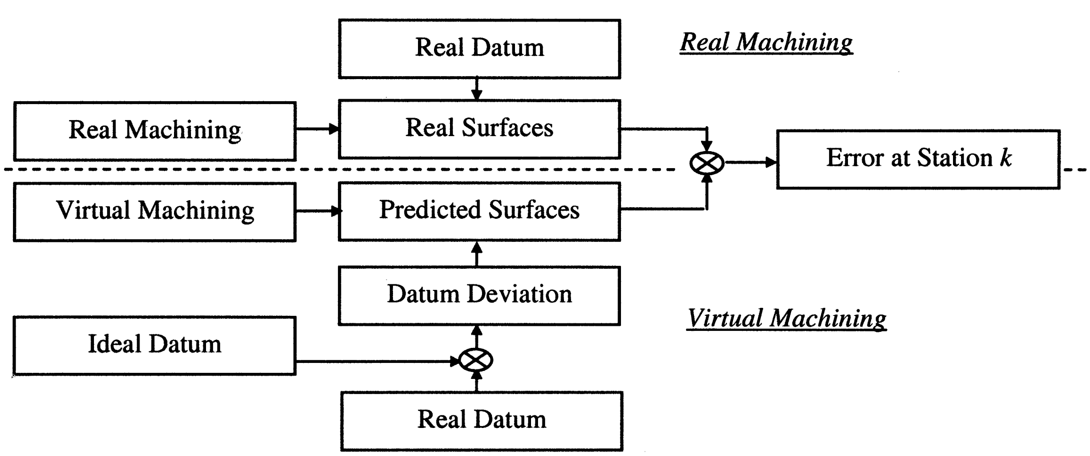

Fig. 3. Variation isolation among operations.

As the machining datum data is available from $\mathbf{y}(k-1)$, $\mathbf{x}^{u'}(k)$ is attainable by Equation (21). We can take n_2 samples of $\mathbf{y}'(k)$ through simulation and compute $\hat{\boldsymbol{\mu}}_{\mathbf{y}'(k)}$ and $\mathbf{S}_{\mathbf{y}'(k)}$.

The faulty operation can be determined by hypothesis testing on the samples from $\mathbf{y}(k)$ and $\mathbf{y}'(k)$. Let $\mathbf{y}(k)$ and $\mathbf{y}'(k)$ be p-variant vectors. For each operation, the hypothesis test procedure is given as follows:

1. $H_0 : \mathbf{K}_{\mathbf{y}(k)} = \mathbf{K}_{\mathbf{y}'(k)}$ vs. $H_1 : \mathbf{K}_{\mathbf{y}(k)} \neq \mathbf{K}_{\mathbf{y}'(k)}$
   If the H_0 hypothesis is rejected at level α, faults are assumed to occur at operation k and we terminate the test. If the H_0 hypothesis fails to be rejected, we go on to the second test in step 2.
   The details of this hypothesis test can be found in Muirhead (1982). A likelihood ratio statistics is defined as:

$$\Lambda_k^* = \frac{\left(\det\left((n_1-1)\mathbf{S}_{\mathbf{y}(k)}\right)\right)^{(n_1-1)/2}\left(\det\left((n_2-1)\mathbf{S}_{\mathbf{y}'(k)}\right)\right)^{(n_2-1)/2}}{\left[\det\left((n_1-1)\mathbf{S}_{\mathbf{y}(k)}+(n_2-1)\mathbf{S}_{\mathbf{y}'(k)}\right)\right]^{(n_1+n_2-2)/2}} \times \frac{(n_1+n_2-2)^{((n_1+n_2-2)/2)P}}{(n_1-1)^{((n_1-1)/2)P}(n_2-1)^{((n_2-1)/2)p}}. \quad (22)$$

   For large $M = \rho(n_1+n_2-2)$ with:

$$\rho = 1 - \frac{2p^2+3p-1}{6(p+1)(n_1+n_2-2)}\left(\frac{n_1-1}{n_2-1}+\frac{n_2-1}{n_1-1}+1\right),$$

   the approximate distribution of the test statistics is:

$$P(-2\rho\log\Lambda_k^* \le x) = P\left(\chi_f^2 \le x\right) + \frac{r}{M^2}\left[P\left(\chi_{f+4}^2 \le x\right) - P\left(\chi_f^2 \le x\right)\right] + O(M^{-3}), \quad (23)$$

   where $P(\chi_f^2 \le x)$ is the chi-square distribution with f degrees of freedom. Here $f = (p(p+1))/2$, and:

$$r = \frac{p(p+1)}{48}\left\{(p-1)(p+2)\left(\frac{n_1-1}{n_2-1}+\frac{n_2-1}{n_1-1}+1\right) - 6\left[(n_1+n_2-2)(1-\rho)\right]^2\right\}.$$

   We reject H_0 if $-2\rho\log\Lambda_k^* > c_f(\alpha)$, where $c_f(\alpha)$ denotes the upper α quantile of the χ_f^2 distribution.
2. $H_0 : \boldsymbol{\mu}_{\mathbf{y}(k)} = \boldsymbol{\mu}_{\mathbf{y}'(k)}$ vs. $H_1 : \boldsymbol{\mu}_{\mathbf{y}(k)} \neq \boldsymbol{\mu}_{\mathbf{y}'(k)}$ with $\mathrm{K}_{\mathbf{y}(k)} = \mathrm{K}_{\mathbf{y}'(k)}$ (unknown covariance).
   If the H_0 hypothesis is rejected at level α, mean shifts are assumed to occur at operation k. If the H_0 hypothesis fails to be rejected, no fault occurs at operation k. We can use Hotelling's T^2 for this hypothesis test. The two-sample T^2-statistic is given by:

$$T^2_{\alpha,p,n_1+n_2-2} = \left(\hat{\boldsymbol{\mu}}_{\mathbf{y}(k)} - \hat{\boldsymbol{\mu}}_{\mathbf{y}'(k)}\right)^T \times\left[\left(\frac{1}{n_1}+\frac{1}{n_2}\right)\frac{(n_1-1)\mathbf{S}_{\mathbf{y}(k)}+(n_2-1)\mathbf{S}_{\mathbf{y}'(k)}}{n_1+n_2-2}\right]^{-1} \times(\hat{\boldsymbol{\mu}}_{\mathbf{y}(k)} - \hat{\boldsymbol{\mu}}_{\mathbf{y}'(k)}), \quad (24)$$

   with $n_1+n_2-2 > p$.

Although the dimension of $\mathbf{y}(k)$ is p, the number of varied components in $\mathbf{y}(k)$ is less than p at each operation because surfaces are not machined only in one operation (for $N > 1$). As a result, $\mathbf{K}_{\mathbf{y}(k)}$ is always a singular matrix. Since hypothesis tests require covariance matrices to be full rank, instead of $\mathbf{y}(k)$, we test its sub-vector, whose components vary in $\mathbf{y}(k)$. More precisely, we reorganize $\mathbf{y}(k)$ and $\mathbf{y}'(k)$ as:

$$\mathbf{y}(k) = [\mathbf{y}^1(k) \mid \mathbf{y}^2(k) \mid \cdots \mid \mathbf{y}^N(k)]^T, \quad (25)$$

$$\mathbf{y}'(k) = [\mathbf{y}^{1'}(k) \mid \mathbf{y}^{2'}(k) \mid \cdots \mid \mathbf{y}^{N'}(k)]^T, \quad (26)$$

where $\mathbf{y}^j(k)$ and $\mathbf{y}^{j'}(k)$ denote the sub-vector affected by operations at operation j.

By definition of $\mathbf{y}^j(k)$ and $\mathbf{y}^{j'}(k)$, it is clear that sub-vectors $\mathbf{y}^k(k)$ and $\mathbf{y}^{k'}(k)$ are sufficient for the hypothesis testing. As a result, we replace $\mathbf{y}(k)$ and $\mathbf{y}'(k)$ with $\mathbf{y}^k(k)$ and $\mathbf{y}^{k'}(k)$ in Equations (22) and (24). p is still used to denote the dimension of the sub-vector.

4. Case study

It is essential to validate the model (Equation (1) before performing variation transmission analysis and process

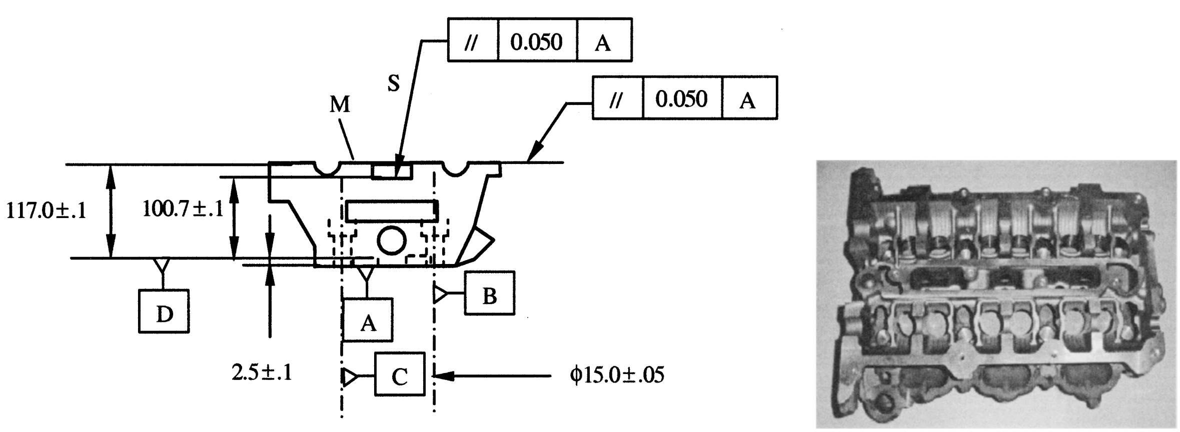

Fig. 4. Design specifications of cylinder head.

Table 1. Description of characteristics

Characteristics	*Specifications, (mm)*	*Operation*
(1) Distance between cover face M and datum surface D	117.0 ± 0.1	1st
(2) Distance between joint face A and datum surface D	2.50 ± 0.1	2nd
(3) Parallelism between M and A	0.050	
(4) Diameter of hole B	15.00 ± 0.05	
(5) Distance between slot S and D	100.7 ± 0.1	3rd
(6) Parallelism between A and S	0.050	

Table 2. Operational sequence and locating datums

Operation	*Locating datums (primary + secondary + tertiary datum)*	*Operation descriptions*
1	$D(T_1, T_2, T_3) + (T_4, T_5) + T_6$	Mill cover M
2	$M1 + (T_4, T_5) + T_6$	Mill joint face A Drill hole B and C
3	$A1 + B + C$	Mill slot S

diagnosis. The model validation has been done in Huang *et al.* (2003) with a V-6 cylinder head as an example, where Coordinate Measuring Machine measurements on machined parts were compared with model predictions under normal and faulty cutting conditions. The comparison results were satisfactory. Validation experiments are also helpful to understand process capabilities.

To illustrate the process-level diagnostics, this section utilizes the same V-6 cylinder head to show the diagnosis procedure. The part and design specifications are shown in Fig. 4.

Descriptions of the characteristics are given in Table 1. The association between characteristics and operations is illustrated by the first and the third column in Table 1.

Three operations are performed to manufacture the part according to the design specifications (Table 2). Figure 5 graphically shows the operational sequence, where the T_i's ($i = 1, 2, \ldots, 6$) are the six locators used as datums. The primary datum surface D consists of T_1, T_2 and T_3. Surface M1 represents the cover face M after the first operation on it. The convention applies to other surfaces.

During simulation studies, faults are purposely introduced into the process. At operation 1, the variations of the fixture locating pins are increased. At operation 2, the heights of the fixture locating pins are increased. Assume that the level of noise is relatively small compared to the variation of the fixture locating pins, e.g., 10 times smaller in the simulation.

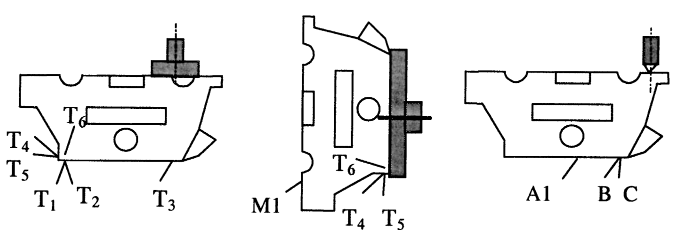

Fig. 5. Operational sequence.

SPC charts are used to show the failure of SPC to identify faulty operation(s). Initially 100 parts are simulated under normal conditions. Then 50 parts are selected for control charting with a sample size of five. For characteristic 5, i.e., "Distance between slot S and D", the X-bar chart and S chart with three sigma control limits are shown in Fig. 6(a and b) respectively. Then 100 parts are simulated under faulty machining conditions. The monitoring results are shown in Fig. 6(c and d). The S-chart in Fig. 6(d) shows eight consecutive points lying one side of the central line and two points out of the upper control limits. This chart indicates that there might be an increase in process variation. The $\bar{X}$ chart in Fig. 6(c) shows all the points lying at one side of the central line and four points out of the upper control limit. This chart indicates that there might be a mean shift in the process. Apparently the process is out of control. However, by analyzing the potential root causes for the characteristic 5, operations are found coupled. There are three candidate operations that could potentially contribute to the out-of-control signal, i.e., operation 3 (because the slot is milled in this operation), operation 2 (because joint face A is machined in operation 2 and will be used as the datum in operation 3), and operation 1 (because the datum used to machine joint face A is machined in operation 1). Thus, the SPC chart fails to distinguish the candidate operations.

The proposed diagnostic is applied to identify the faulty operation(s). The six characteristics are divided into three sub-vectors ($\mathbf{y}^k(k)$) as shown in Table 3. It is easy to prove that the process is diagnosable by Result 3. Then

Table 3. Sub-vector $\mathbf{y}^k(k)$

Operation k	$\mathbf{y}^k(k)$	*Characteristics of interest*	*p*
1	$\mathbf{y}^1(1)$	Distance between cover face M to surface D	1
2	$\mathbf{y}^2(2)$	Distance between joint face A and surface D Parallelism between M and A Diameter of hole B	3
3	$\mathbf{y}^3(3)$	Distance between slot S and D Parallelism between A and S	2

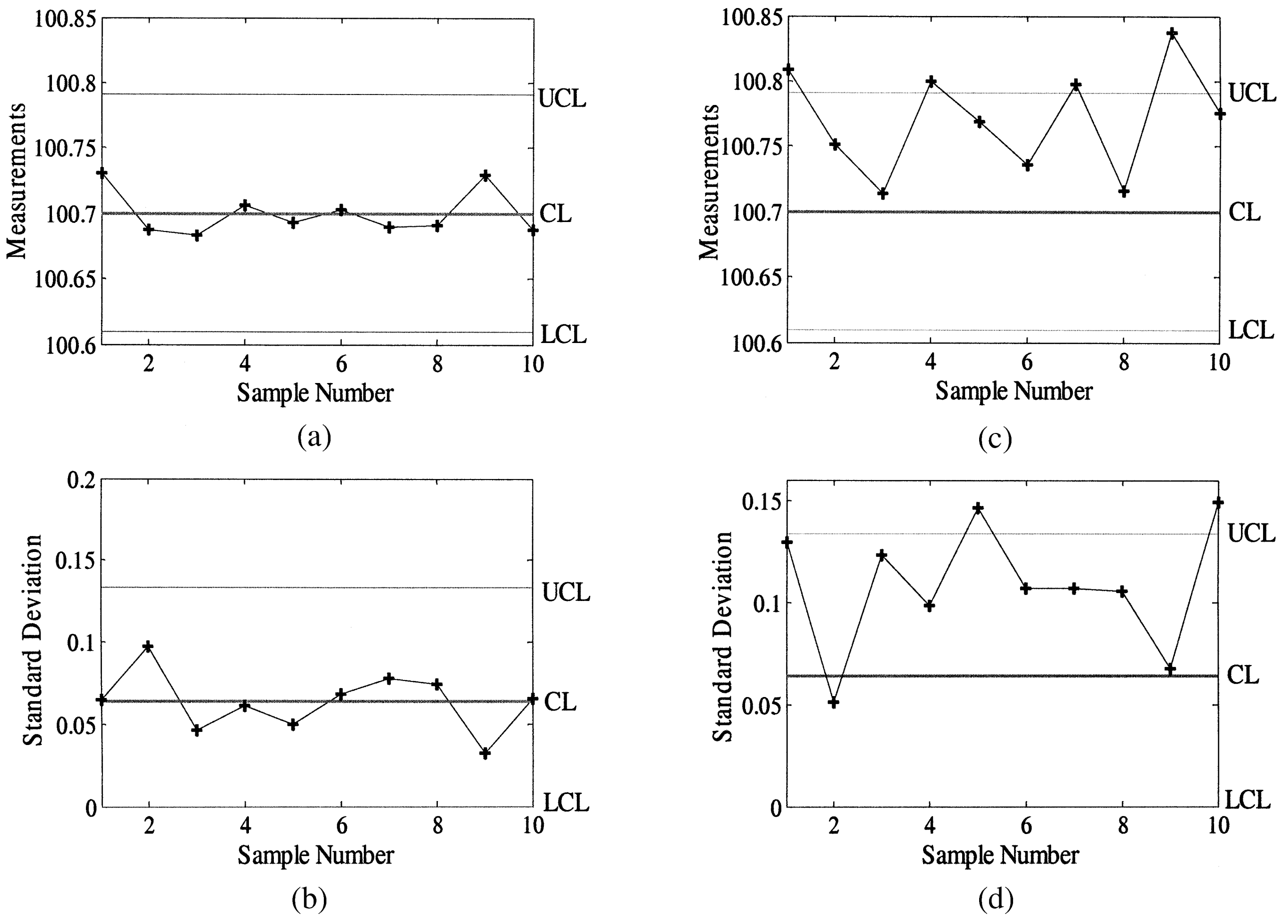

Fig. 6. Simulation results for characteristic 5: (a) the X-bar chart under normal conditions; (b) the S-chart under normal conditions; (c) The X-bar chart under faulty conditions; and (d) the S-chart under faulty conditions.

collect 50 parts under faulty machining conditions. With sample information about machining datums, virtual machining is performed to generate 50 virtual parts. Set level $\alpha = 0.05$, and conduct hypothesis test to identify the faulty operation(s).

The results are shown in Table 4. The hypothesis testing correctly identifies that variation changes in the first operations ($39.545 > 3.8415$). Because of this, the mean test is unnecessary for operation 1. A mean shift is identified at the second operation ($27.2155 > 8.2574$), while operation 3 is found to be stable ($0.04076 < 7.8147$ and $0.0353 < 6.2389$). Although the three operations are coupled, the proposed diagnostic is able to identify faulty operations among three potential faults.

5. Summary

In this paper, variation transmission in MMPs is analyzed based on a state space model. The part variation at each operation is explicitly divided into five components: (i) the variation of uncut surfaces from previous operations; (ii) the variations of machined surfaces due to the current cutting operation; (iii) the fixture; (iv) the datums; and (v) the natural process variation. This result is very helpful for both design and manufacturing, such as in the evaluation of alternative fixture designs or the optimization of the operational sequence.

Based on the variation transmission analysis, a methodology is developed to identify faulty operations in the MMP.

Table 4. Hypothesis testing results

	Operation 1		*Operation 2*		*Operation 3*	
	Covariance test	*Mean test*	*Covariance test*	*Mean test*	*Covariance test*	*Mean test*
Test statistics	39.545	N/A	9.0937	27.2155	0.040 76	0.0353
Threshold	3.8415	N/A	12.5916	8.2574	7.8147	6.2389

Variation isolation among operations is performed based on the concept of virtual machining. The hypothesis testing successfully identifies faulty operations. The conditions for a MMP to be diagnosable are also addressed.

Acknowledgements

The authors gratefully acknowledge the financial support of the NSF Engineering Research Center for Reconfigurable Machining Systems (NSF grant EEC95-92125) at the University of Michigan and the valuable input from the Center's industrial partners.

References

Agrawal, R., Lawless, J.F. and Mackay, R.J. (1999) Analysis of variation transmission in manufacturing processes—part II. *Journal of Quality Technology*, **31**, 143–154.

Anjanappa, M., Anand, D.K., Kirk, J.A. and Shyam, S. (1988) Error correction methodologies and control strategies for numerical machines. *Control Methods for Manufacturing Process*, **7**, 41–49.

Apley, D.W. and Shi, J. (1998) Diagnosis of multiple fixture faults in panel assembly. *ASME Transactions, Journal of Manufacturing Science and Engineering*, **120**, 793–801.

Cai, W., Hu, S.J. and Yuan, J.X. (1997) Variational method of robust fixture configuration design for 3-D workpiece. *ASME Transactions, Journal of Manufacturing Science and Engineering*, **119**, 593–602.

Ceglarek, D. and Shi, J. (1996) Fixture failure diagnosis for the autobody assembly using pattern recognition. *ASME Transactions, Journal of Engineering for Industry*, **118**, 55–66.

Chase, K.W. and Greenwood, W.H. (1988) Design issues in mechanical tolerance analysis. *Manufacturing Review*, **1**, 50–59.

Chen, J.S., Yuan, J.X., Ni, J. and Wu., S.M. (1993) Real-time compensation for time-variant volumetric errors on a machining center. *ASME Transactions, Journal of Engineering for Industry*, **115**, 472–479.

Choudhuri, S.A. and De Meter, E.C. (1999) Tolerance analysis of machining fixture locators. *ASME Transactions, Journal of Manufacturing Science and Engineering*, **121**, 273–281.

Ding, Y., Ceglarek, D. and Shi, J. (2002) Fault diagnosis of multistage manufacturing processes by using state space approach. *ASME Transactions, Journal of Manufacturing Science and Engineering*, **124**, 313–322.

Djurdjanovic, D. and Ni, J. (2001) Linear state space modeling of dimensional machining errors. *NAMRI/SME*, **XXIX**, 541–548.

Huang, Q., Shi, J. and Yuan, J. (2003) Part dimensional error and its propagation modeling in multi-operational machining processes. *ASME Transactions, Journal of Manufacturing Science and Engineering*, **125**, 255–262.

Huang, Q., Zhou, N. and Shi, J. (2000) Stream-of-variation modeling and diagnosis of multi-station machining processes, in *Proceedings of the International Mechanical Engineering 2000 ASME Congress & Exposition*, Orlando, FL, Vol. **11**, pp. 81–88.

Huang, Q., Zhou, S. and Shi, J. (2002) Diagnosis of multi-operational machining processes through process analysis. *Robotics and Computer-Integrated Manufacturing*, **18**, 233–239.

Jin, J. and Shi, J. (1999) State space modeling of sheet metal assembly for dimensional control. *ASME Transactions, Journal of Manufacturing Science and Engineering*, **121**, 756–762.

Lawless, J.F., MacKoy, R.J. and Robinson, J.A. (1999) Analysis of variation transmission in manufacturing processes—Part I. *Journal of Quality Technology*, **31**, 131–142.

Mantripragada, R. and Whitney, D.E. (1999) Modeling and controlling variation propagation in mechanical assemblies using state transition models. *IEEE Transactions on Robotics and Automation*, **15**, 124–140.

Muirhead, R.J. (1982) *Aspects of Multivariate Statistical Theory*, Wiley, New York, NY.

Rong, Y. and Bai, Y. (1996) Machining accuracy analysis for computer-aided fixture design verification. *ASME Transactions, Journal of Manufacturing Science and Engineering*, **118**, 289–299.

Shi, J. and Jin, J. (1997) Modeling and diagnosis for automotive body assembly process using state space models, *in Proceedings of the International Conference on Intelligent Manufacturing Systems*, 97 pp. 189–196, Seoul, Korea.

Wade, M.R. and Woodall, W.H. (1993) A review and analysis of cause-selecting control charts. *Journal of Quality Technology*, **25**, 161–168.

Weil, R., Darel, I. and Laloum, M. (1991) The influence of fixture positioning errors on the geometric accuracy of mechanical parts, in *Proceedings of the CIRP Conference on PE & MS*, Tianjin, China, pp. 215–225.

Zhang, G.X. (1984) New type of quality control charts—cause-selecting control charts and a theory of diagnosis with control charts, in *Proceedings of the World Quality Congress '84*, London, pp. 75–185.

Zhou, S., Huang, Q. and Shi, J. (2003) State space modeling for dimensional monitoring of multistage machining process using differential motion vector. *IEEE Transactions on Robotics and Automation*, **19**, 296–309.

Biographies

Qiang Huang received B.S., M.S. and Ph.D. degrees in Mechanical Engineering from the Shanghai JiaoTong University in 1993, 1996 and 1998, respectively. He also received a Ph.D. degree in Industrial and Operations Engineering from the University of Michigan in 2003. He is currently an Assistant Professor in the Department of Industrial and Management Systems Engineering at the University of South Florida. His research interests are centered on variation reduction for complex manufacturing processes, integrated design and manufacturing, and engineering statistics. He received the 2002–2003 Student of the Year award at the NSF Engineering Research Center for Reconfigurable Machining Systems at the University of Michigan. He is a member of IIE, INFORMS, ASME, and SME.

Jianjun Shi received his B.S. and M.S. in Electrical Engineering at the Beijing Institute of Technology in 1984 and 1987 respectively, and his Ph.D. in Mechanical Engineering at the University of Michigan in 1992. He is currently a Professor in the Department of Industrial and Operations Engineering at the University of Michigan. His research interests are the fusion of advanced statistics and engineering knowledge to develop in-process quality improvement methodologies achieving automatic process monitoring, diagnosis, compensation, and their implementation in various manufacturing processes. He has received numerous awards and currently serves as a Department Editor of *IIE Transactions on Quality and Reliability*. He is a member of IIE, INFORMS, ASME, ASQC and SME.

Contributed by the On-Line Quality Engineering Department